Available online at www.sciencedirect.com
SCIENCE DIRECT®
Journal of Sound and Vibration 272 (2004) 831–851
JOURNAL OF SOUND AND VIBRATION
www.elsevier.com/locate/jsvi

Free in-plane vibration analysis of rectangular plates by the method of superposition

D.J. Gorman*

Department of Mechanical Engineering, University of Ottawa, 770 King Edward Avenue, Ottawa, Ont., Canada K1N 6N5

Received 28 October 2002; accepted 31 March 2003

Abstract

The superposition method is introduced as a means for obtaining analytical-type solutions for free in-plane vibration of rectangular plates. The governing differential equations and boundary conditions are expressed in dimensionless form. The problem of free in-plane vibration of the completely free rectangular plate is resolved for illustrative purposes. Convergence is found to be rapid and excellent agreement between computed results and those obtained by previous authors utilizing the Rayleigh–Ritz energy method is obtained. It is pointed out that following procedures analogous to those utilized in resolving lateral plate vibration problems, in-plane free vibration problems related to point supported plates, plates with in-plane elastic boundary support, etc., are now amenable to solution by this method.
© 2003 Elsevier Ltd. All rights reserved.

1. Introduction

A vast array of technical papers related to the free lateral vibration of rectangular plates has been available in the literature for a number of years. Each year further technical papers related to this subject matter appear in the technical journals.

The situation with regard to free in-plane vibration of these plates is quite different. Here, it is recognized that the results of only a minuscule number of studies have been published. A number of these are to be found listed in Ref. [1]. It is generally agreed that this discrepancy is due to the fact that natural frequencies of plates in lateral vibration are invariably much lower than those of plates in in-plane vibration. The lateral vibration modes are therefore much more likely to be excited by the time-varying forces normally available to provide this excitation.

*Tel.: +1-613-562-5800; fax: +1-613-562-5177.
E-mail address: dgorman@genie.uottawa.ca (D.J. Gorman).

0022-460X/03/$ - see front matter © 2003 Elsevier Ltd. All rights reserved.
doi:10.1016/S0022-460X(03)00421-8

In more recent studies, particularly those related to ship hull design, it is found that a strong relationship between plate in-plane vibration and high-frequency noise can exist. This has led to a renewed interest in the phenomenon of rectangular plate in-plane vibration. It should also be pointed out that plates subjected to fluid turbulent boundary layers can, in fact, be excited in both in-plane and transverse vibration modes. It is found, furthermore, that due to the nature of the in-plane problem and its elevated natural frequencies, the analysis of such problems by the finite element method becomes difficult.

For these reasons it has been decided to explore the applicability of the superposition method as a means for analyzing rectangular plate in-plane free vibration problems. This method, which has found such wide application in analysis of plate lateral free vibration, is introduced here as a powerful means of obtaining analytical-type solutions for the in-plane problem. Among its advantages are the fact that no mode shapes need be selected, as is the case for the Rayleigh–Ritz energy approach. The governing differential equations are satisfied exactly throughout the domain of the plate. Boundary conditions are satisfied to any desired degree of accuracy.

For development of the analytical technique, and illustration of its capabilities, attention is focused on the classical problem of free in-plane vibration of the completely free rectangular plate. Exact solutions are known to exist for plates with what are defined as simply supported edge conditions.

It will become apparent to the reader that, in fact, this self-contained method not only works extremely well for the completely free plate problem but it is ideally suited for handling plates with various combinations of boundary conditions, fixed point supports, etc. Computed results will be compared with those of Badell et al. [1]. They have examined the in-plane free vibration of plates with classical edge conditions by means of the Rayleigh–Ritz approach. They have employed what are described as 'an ascending hierarchy of K-orthogonal polynomials in conjunction with Hermite cubics' to represent plate in-plane displacement.

Kobayshi et al. [2] have examined the problem of in-plane vibration of rectangular plates with point supports. Plate deflections were expressed in series utilizing the product of power functions and the Ritz method was employed to obtain a solution. Gutierrez and Laura [3] examined in-plane free vibration of rectangular plates with in-plane elastic support at the boundaries. They used an extension of the method employed by Mikhlin to obtain the lowest frequency of completely free plate vibration. What is described as 'an approximate solution' was obtained by the Ritz approach.

It may be appropriate to repeat here that, in what is to follow, the challenge of trying to select appropriate functions to represent plate displacements is completely eliminated.

2. Mathematical procedure

Utilizing conventional notation the well-known dynamic equilibrium equations governing the in-plane vibration of a rectangular plate are written as

$$\frac{\partial \sigma_x}{\partial x} + \frac{\partial \tau_{xy}}{\partial y} = \rho \frac{\partial^2 u}{\partial t^2} \tag{1}$$

and

$$\frac{\partial \tau_{xy}}{\partial x} + \frac{\partial \sigma_y}{\partial y} = \rho \frac{\partial^2 v}{\partial t^2}, \tag{2}$$

where ρ is the density of the plate material, u, and v, represent motion in the x and y directions, respectively, and t represents time.

The stresses are written as

$$\sigma_x = A_{11}\frac{\partial u}{\partial x} + A_{12}\frac{\partial v}{\partial y}, \qquad \sigma_y = A_{12}\frac{\partial u}{\partial x} + A_{22}\frac{\partial v}{\partial y}, \qquad \tau_{xy} = A_{66}\left\{\frac{\partial v}{\partial x} + \frac{\partial u}{\partial y}\right\},$$

where $A_{11} = A_{22} = E/(1-v^2)$, $A_{12} = vE/(1-v^2)$, and $A_{66} = G_{xy}$.

Here v and E are the material Poisson ratio, and Young's modulus, respectively, and G_{xy} is the modulus of elasticity is shear.

Utilizing the above stress–displacement relationships and substituting in the equilibrium equations (1) and (2) we obtain

$$A_{11}\frac{\partial^2 u}{\partial x^2} + A_{12}\frac{\partial^2 v}{\partial x \partial y} + A_{66}\left\{\frac{\partial^2 v}{\partial x \partial y} + \frac{\partial^2 u}{\partial y^2}\right\} = \rho \frac{\partial^2 u}{\partial t^2} \tag{3}$$

and

$$A_{66}\left\{\frac{\partial^2 v}{\partial x^2} + \frac{\partial^2 u}{\partial x \partial y}\right\} + A_{12}\frac{\partial^2 u}{\partial x \partial y} + A_{22}\frac{\partial^2 v}{\partial y^2} = \rho \frac{\partial^2 v}{\partial t^2}, \tag{4}$$

This is an alternative form of the equilibrium equations and the one that will be utilized here.

Consider a plate with edge length 'a' running in the x direction and edge length 'b' running in the y direction (see Fig. 1). In order to develop the equilibrium equations in dimensionless form we will divide the plate in-plane displacements u, and v, by edge length 'a', and denote the dimensionless displacements by the symbols U and V, respectively (Fig. 1) . We also introduce the dimensionless co-ordinates $\xi = x/a$, and $\eta = y/b$. The variables U and V represent amplitude of harmonic motions of circular frequency ω. Substituting the above dimensionless quantities in Eqs. (3) and (4) it is then readily shown that these equations may be expressed in dimensionless form as

$$a_{11}\frac{\partial^2 U}{\partial \xi^2} + \frac{a_{12}}{\phi}\frac{\partial^2 V}{\partial \xi \partial \eta} + \frac{a_{66}}{\phi}\left\{\frac{\partial^2 V}{\partial \xi \partial \eta} + \frac{1}{\phi}\frac{\partial^2 U}{\partial \eta^2}\right\} + \lambda^4 U = 0 \tag{5}$$

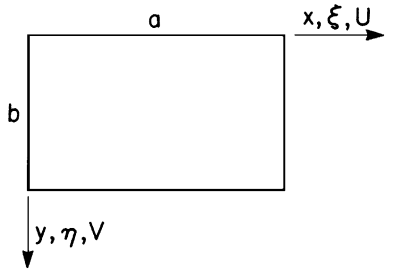

Fig. 1. Schematic representation of completely free rectangular plate to be analyzed.

and

$$a_{66}\left\{\frac{\partial^2 V}{\partial \xi^2}+\frac{1}{\phi}\frac{\partial^2 U}{\partial \xi \partial \eta}\right\}+\frac{a_{12}}{\phi}\frac{\partial^2 U}{\partial \eta \partial \xi}+\frac{a_{11}}{\phi^2}\frac{\partial^2 V}{\partial \eta^2}+\lambda^4 V=0, \tag{6}$$

where φ equals the plate aspect ratio, b/a, and the dimensionless frequency is λ^2 where $\lambda^2 = \omega a\sqrt{\rho(1-\nu^2)/E}$. The quantities $a_{11}=1$, $a_{12}=\nu$, and $a_{66}=(1-\nu)/2$.

The dimensionless equilibrium equations (5) and (6) are utilized in all work reported here.

It is appropriate at this time to introduce dimensionless stresses, σ_y^*, σ_x^*, and τ_{xy}^*. Beginning with expressions provided for stresses earlier we have

$$\sigma_y=\frac{\nu E}{1-\nu^2}\frac{\partial u}{\partial x}+\frac{E}{1-\nu^2}\frac{\partial v}{\partial y} \quad \text{or} \quad \frac{\sigma_y(1-\nu^2)}{E}=\nu\frac{\partial u}{\partial x}+\frac{\partial v}{\partial y}$$

and

$$\sigma_y^*=\frac{\sigma_y(1-\nu^2)}{E} \quad \text{or} \quad \sigma_y^*=\nu\frac{\partial U}{\partial \xi}+\frac{1}{\phi}\frac{\partial V}{\partial \eta}. \tag{7}$$

Similarly, we obtain

$$\sigma_x^*=\frac{\sigma_x(1-\nu^2)}{E} \quad \text{or} \quad \sigma_x^*=\frac{\partial U}{\partial \xi}+\frac{\nu}{\phi}\frac{\partial V}{\partial \eta}. \tag{8}$$

Rearranging the expression provided for τ_{xy} we have

$$\frac{\tau_{xy}}{A_{66}}=\frac{\partial V}{\partial \xi}+\frac{1}{\phi}\frac{\partial U}{\partial \eta}.$$

Then we set

$$\tau_{xy}^*=\frac{\tau_{xy}\phi}{A_{66}} \quad \text{or} \quad \tau_{xy}^*=\frac{\partial U}{\partial \eta}+\phi\frac{\partial V}{\partial \xi}. \tag{9}$$

We are now in a position to begin the in-plane vibration analysis of rectangular plates. We wish at this time to focus attention on the completely free plate. Such a plate is depicted in Fig. 2 where the reference axes coincide with the plate central axes. In fact, it will become apparent that we need only focus attention on the quarter plate bounded by the ξ- and η-axis. For our plate

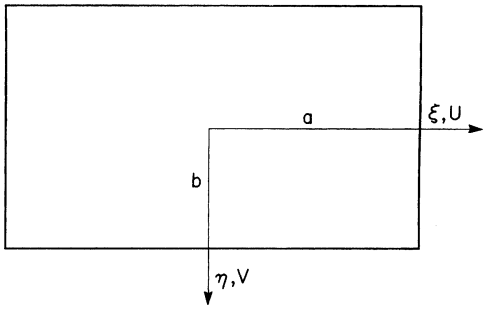

Fig. 2. The completely free plate with central co-ordinate axes.

dimensions a, and b, referred to earlier, we will utilize the dimensions of the quarter plate as indicated in the figure.

It will be appreciated that a certain amount of symmetry, or anti-symmetry, of plate in-plane displacements about the plate central axes is to be expected for each plate free vibration mode shape. We choose to define a free vibration mode as being symmetric about an axis if displacement normal to this axis has a symmetric distribution about it.

Referring to the ξ-axis of the quarter plate it is to be anticipated that for any free vibration mode, displacement normal to this axis, i.e., displacement V, will either be symmetrically, or anti-symmetrically, distributed about this axis. In the case of a symmetric distribution we will have, $\partial V/\partial\eta = 0$, along the ξ-axis. Conversely, if we have an anti-symmetric distribution we will have, $V = 0$, along the same axis.

It will be appreciated that completely analogous constraints on the displacement U can be written with regard to the η-axis.

For the completely free plate we need only analyze the quarter plate of Fig. 2, provided all possible modes are analyzed. We define those mode families as follows:

Symmetric–symmetric modes: Displacement normal to each axis of the quarter plate will be symmetrically distributed with respect to these axes.

Anti-symmetric–anti-symmetric modes: Displacement normal to each of the above axes will be anti-symmetrically distributed with respect to these axes.

Symmetric–anti-symmetric modes: Displacement normal to the ξ-axis will be symmetrically distributed with respect to this axis while displacement normal to the η-axis will be anti-symmetrically distributed with respect to this axis.

In the work to follow each of the above families of modes will be analyzed separately and will be referred to utilizing the designations introduced above. In this way all of the in-plane vibration modes of the completely free plate will be established. Furthermore, the three characteristic mode families will be clearly separated out. This constitutes a continuation of a similar approach which was introduced for the lateral free vibration analysis of the completely free plate [4].

We are now in a position to begin analysis of the three in-plane free vibration mode families discussed above.

2.1. The symmetric–symmetric mode family

Consider the quarter plate as shown on the left hand side of Fig. 3. Pairs of small circles adjacent to the edges, $\xi = 0$, and $\eta = 0$, indicate that conditions of symmetry, as discussed above, are to be satisfied along these edges. The other edges of the quarter plate are free of surface tractions.

In the procedure to follow it will be shown how a solution for the free in-plane vibration modes and frequencies of the quarter plate is obtained by first superimposing the two edge driven in-plane forced vibration problems (building blocks) shown schematically to the right of the figure. In a manner completely analogous to that followed in the analysis of lateral free vibration of the same plate, free vibration eigenvalues are obtained by constraining Fourier driving coefficients appearing in the distributed edge-driving forces. These coefficients are constrained so as to insure that boundary conditions required of the superimposed set are satisfied.

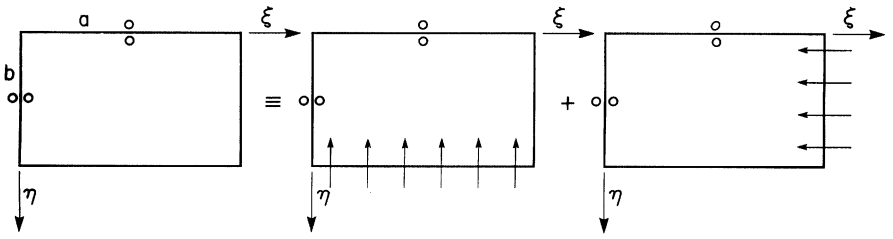

Fig. 3. Schematic representation of quarter plate under study and building blocks utilized in symmetric–symmetric mode analysis. Adjacent short arrows indicate amplitude of distributed in-plane forces acting on driven edges.

Consider now the first building block on the right hand side of the figure. Conditions of zero in-plane shear stress are to be enforced along the edges, $\xi = 1$, and $\eta = 1$. A distributed harmonic driving force is to be imposed along the edge, $\eta = 1$.

We take the solution for the amplitude of harmonic displacements of this building block as follows:

$$U(\xi,\eta) = \sum_{m=1,2}^{\infty} U_m(\eta)\cos(2m-1)\frac{\pi\xi}{2} \tag{10}$$

and

$$V(\xi,\eta) = \sum_{m=1}^{\infty} V_m(\eta)\sin(2m-1)\frac{\pi\xi}{2}. \tag{11}$$

This is a Levy-type solution. The prescribed boundary conditions are satisfied along edges at the extremities of the Fourier trigonometric functions, as required of all Levy-type solutions. It will be noted that since the quantity $U(\xi,\eta)$ equals zero along the edge, $\xi = 1$, the quantity $\partial U(\xi,\eta)/\partial\eta$ will also equal zero, as does the quantity $\partial V(\xi,\eta)/\partial\xi$. Shear forces along this edge are therefore zero (Eq. (9)).

Substituting Eqs. (10) and (11) into the equilibrium equations (5) and (6), it is readily shown that we obtain

$$a_{m1}U_m''(\eta) + b_{m1}V_m'(\eta) + C_{m1}U_m(\eta) = 0 \tag{12}$$

and

$$a_{m2}V_m''(\eta) + b_{m2}U_m'(\eta) + c_{m2}V_m(\eta) = 0, \tag{13}$$

where superscripts imply differentiation with respect to the variable η and

$$a_{m1} = \frac{a_{66}}{\phi^2}, \quad b_{m1} = \frac{emp}{\phi}(a_{12}+a_{66}), \quad c_{m1} = -a_{11}emps + \lambda^4, \quad a_{m2} = \frac{a_{11}}{\phi^2},$$

$$b_{m2} = \frac{-emp}{\phi}(a_{66}+a_{12}), \quad C_{m2} = -a_{66}emps + \lambda^4.$$

Here, in the interest of brevity, symbols 'emp' and 'emps' are introduced to represent quantities $(2m-1)\pi/2$, and $\{(2m-1)\pi/2\}^2$, respectively.

The quantities $U_m^{|}(\eta)$, and $U_m^{||||}(\eta)$, may be expressed in terms of the parameter $V_m(\eta)$ and its derivatives, by means of Eq. (13). Turning to Eq. (12), differentiating it once with respect to η, and then replacing the quantities $U_m^{|}(\eta)$ and $U_m^{||||}(\eta)$ with the above expressions, we obtain the following fourth order homogeneous differential equation involving the quantity $V_m(\eta)$ only:

$$V_m^{iv}(\eta) + bV_m''(\eta) + cV_m(\eta) = 0, \tag{14}$$

where

$$b = (a_{m1}c_{m2} - b_{m1}b_{m2} + c_{m1}a_{m2})/a_{m1}a_{m2}$$

and

$$c = c_{m1}c_{m2}/a_{m1}a_{m2}.$$

Focusing on the differential equation (14) and denoting the square of the roots of the characteristic equation associated with it as ε^2, we may write

$$(\varepsilon^2)^2 + b\varepsilon^2 + c = 0. \tag{15}$$

The roots for ε^2, denoted as ε_1^2 and ε_2^2, become

$$\varepsilon_1^2 = \frac{-b + \sqrt{b^2 - 4c}}{2}, \quad \varepsilon_2^2 = \frac{-b - \sqrt{b^2 - 4c}}{2}.$$

It is found in all the work reported here that the quantity $b^2 - 4c$ is positive. This means that the quantities ε_1^2 and ε_2^2 are real, though they may be positive or negative. We denote these quantities as $Root1$, and $Root2$, respectively. We also introduce the quantities $\beta_m = \sqrt{|Root1|}$ and $\gamma_m = \sqrt{|Root2|}$. Three forms of solution for Eq. (14) are therefore possible, as follows:

Solution 1: $Root1 \geqslant 0$, $Root2 \leqslant 0$; then

$$V_m(\eta) = A_m \sinh \beta_m\eta + B_m \cosh \beta_m(\eta) + C_m \sin \gamma_m(\eta) + D_m \cos \gamma_m\eta, \tag{16}$$

where A_m, B_m, etc., are constants to be determined.

Solution 2: $Root1 \leqslant 0$, $Root2 \leqslant 0$

$$V_m(\eta) = A_m \sin \beta_m\eta + B_m \cos \beta_m(\eta) + C_m \sin \gamma_m\eta + D_m \cos \gamma_m\eta. \tag{17}$$

Solution 3: $Root1 \geqslant 0$, $Root2 \geqslant 0$

$$V_m(\eta) = A_m \sinh \beta_m\eta + B_m \cosh \beta_m\eta + C_m \sinh \gamma_m\eta + D_m \cosh \gamma_m\eta. \tag{18}$$

We return now to obtaining the forced vibration response of the first building block of Fig. 3. We will provide expressions for the response associated with each of the above solution forms separately.

Case 1: Solution 1 applicable. In view of the symmetry in the distribution of the displacement $V(\xi, \eta)$ with respect to the ξ axis, we write

$$V_m(\eta) = B_m \cosh \beta_m\eta + D_m \cos \gamma_m\eta. \tag{19}$$

It will be noted that terms in the quantity $V_m(\eta)$, anti-symmetric with respect to the ξ-axis, have been deleted.

We next focus on the quantity $U_m(\eta)$. Utilizing Eq. (12) we can express $U_m(\eta)$ in terms of $U_m^{||}(\eta)$ and $V_m^{|}(\eta)$. But Eq. (13) permits us to express $U_m^{||}(\eta)$ in terms of $V_m^{||||}(\eta)$ and $V_m^{|}(\eta)$. Combining these two relationships we are able to express the quantity $U_m(\eta)$ in terms of the derivatives of the

quantity $V_m(\eta)$. Utilizing Eq. (19) we then obtain

$$U_m(\eta) = B_m\alpha_{2m}\sinh\beta_m\eta + D_m\alpha_{4m}\sin\gamma_m\eta, \tag{20}$$

where

$$\alpha_{2m} = \beta_m\{a_{m1}a_{m2}\beta_m^2 + a_{m1}c_{m2} - b_{m1}b_{m2}\}/c_{m1}b_{m2}$$

and

$$\alpha_{4m} = \gamma_m\{a_{m1}a_{m2}\gamma_m^2 - a_{m1}c_{m2} + b_{m1}b_{m2}\}/c_{m1}c_{m2}.$$

Note that the quantity $U_m(\eta)$ will have a distribution which is anti-symmetric with respect to the ξ-axis.

It will be recalled that the driven edge of the building block is free of in-plane shear stress. We therefore enforce the edge condition (Eq. (9))

$$\frac{\partial U_m(\eta)}{\partial\eta} + \phi\frac{\partial V_m(\eta)}{\partial\xi}\bigg|_{\eta=1} = 0. \tag{21}$$

Enforcing this boundary condition to evaluate the coefficient D_m we obtain

$$V_m(\eta) = B_m\{\cosh\beta_m\eta + \theta_{1m}\cos\gamma_m\eta\} \tag{22}$$

and

$$U_m(\eta) = B_m\{\alpha_{2m}\sinh\beta_m\eta + \theta_{1m}\alpha_{4m}\sin\gamma_m\eta\}, \tag{23}$$

where

$$\theta_{1m} = \frac{-\{\alpha_{2m}\beta_m + \phi\, emp\}\cosh\beta_m}{\{\alpha_{4m}\gamma_m + \phi\, emp\}\cos\gamma_m}.$$

Finally, we must enforce the condition of dynamic equilibrium along the edge, $\eta = 1$, where the distributed in-plane harmonic driving force is imposed.

Let the spatial distribution of the amplitude of the imposed normal stress be represented in series form as

$$\sigma_y^* = \sum_{m=1,2}^{\infty} E_m\sin emp\,\xi. \tag{24}$$

Substituting Eqs. (22) and (23) into Eq. (7), and utilizing the equality expressed by Eq. (24), the unknown coefficient B_m is readily expressed in terms of the driving coefficient, E_m, for any value of m.

This permits us to write the quantities $V_m(\eta)$, and $U_m(\eta)$ as

$$V_m(\eta) = E_m\theta_{11m}\{\cosh\beta_m\eta + \theta_{1m}\cos\gamma_m\gamma\} \tag{25}$$

and

$$U_m(\eta) = E_m\theta_{11m}\{\alpha_{2m}\sinh\beta_m\eta + \theta_{1m}\alpha_{4m}\sin\gamma_m\eta\}, \tag{26}$$

where

$$\theta_{11m} = \frac{1}{\{[\beta_m/\phi - v\, emp\,\alpha_{2m}]\sinh\beta_m - \theta_{1m}[\gamma_m/\phi + v\, emp\,\alpha_{4m}]\sin\gamma_m\}}.$$

Referring to Eqs. (10) and (11), it is seen that we now have available the building block response to any harmonic normal stress imposed along its driven edge, provided Solution 1 is applicable. It will be appreciated that an identical procedure will be followed in order to obtain expressions for the response when either of the other two solution forms are applicable. There is no need to give a detailed description of these procedures here. Only the expressions required to describe the building block response associated with each of these two solution forms will be provided. Only the quantities $U_m(\eta)$ and $V_m(\eta)$ of Eqs. (10) and (11) will be different.

Case 2: Solution 2 applicable

$$V_m(\eta) = E_m\theta_{11m}\{\cos\beta_m\eta + \theta_{1m}\cos\gamma_m\eta\} \tag{27}$$

and

$$U_m(\eta) = E_m\theta_{11m}\{\alpha_{2m}\sin\beta_m\eta + \theta_{1m}\alpha_{4m}\sin\gamma_m\eta\}, \tag{28}$$

where

$$\theta_{11m} = \frac{-1}{\{[\beta_m/\phi + \nu\, emp\,\alpha_{2m}]\sin\beta_m + \theta_{1m}[\gamma_m/\phi + \nu\, emp\,\alpha_{4m}]\sin\gamma_m\}},$$

$$\theta_{1m} = \frac{-(\alpha_{2m}\beta_m + \phi\, emp)\cos\beta_m}{(\alpha_{4m}\gamma_m + \phi\, emp)\cos\gamma_m},$$

$$\alpha_{2m} = \beta_m\{a_{m1}a_{m2}\beta_m^2 - a_{m1}c_{m2} + b_{m1}b_{m2}\}/c_{m1}b_{m2},$$

$$\alpha_{4m} = \gamma_m\{a_{m1}a_{m2}\gamma_m^2 - a_{m1}c_{m2} + b_{m1}b_{m2}\}/c_{m1}b_{m2}.$$

Case 3: Solution 3 applicable

$$V_m(\eta) = E_m\theta_{11m}\{\cosh\beta_m\eta + \theta_{1m}\cosh\gamma_m\eta\} \tag{29}$$

and

$$U_m(\eta) = E_m\theta_{11m}\{\alpha_{2m}\sinh\beta_m(\eta) + \theta_{1m}\alpha_{4m}\sinh\gamma_m\eta\}, \tag{30}$$

where

$$\theta_{11m} = \frac{1.}{\{[\beta_m/\phi - \nu\, emp\,\alpha_{2m}]\sinh\beta_m + \theta_{1m}[\gamma_m/\phi - \nu\, emp\,\alpha_{4m}]\sinh\gamma_m\}},$$

$$\theta_{1m} = \frac{-[\alpha_{2m}\beta_m + \phi\, emp]\cosh\beta_m}{[\alpha_{4m}\gamma_m + \phi\, emp]\cosh\gamma_m},$$

$$\alpha_{2m} = \beta_m[a_{m1}a_{m2}\beta_m^2 + a_{m1}c_{m2} - b_{m1}b_{m2}]/c_{m1}b_{m2},$$

$$\alpha_{4m} = \gamma_m[a_{m1}a_{m2}\gamma_m^2 + a_{m1}c_{m2} - b_{m1}b_{m2}]/c_{m1}b_{m2}.$$

The entire solution is therefore available for the response of the first building block of Fig. 3.

We turn next to obtaining the solution of the second building block. It differs from the first only in that it is driven along the edge, $\xi = 1$, and a condition of zero shear stress is imposed along the edge, $\eta = 1$. It will be apparent that the solution for the response of this second building block is readily extracted from that of the first. In order to avoid confusion the symbol 'n' rather than 'm' is now utilized in designating the terms in the series summations.

We still wish to use the symbols U and V to indicate displacement parallel to the ξ- and η-axis, respectively. After interchange of the variables ξ and η, we write for the response of this building block (see Eqs. (10) and (11))

$$U(\xi,\eta)=\sum_{n=1,2}^{\infty} U_n(\xi)\sin(2n-1)\frac{\pi\eta}{2} \tag{31}$$

and

$$V(\xi,\eta)=\sum_{n=1,2}^{\infty} V_n(\xi)\cos(2n-1)\frac{\pi\eta}{2}. \tag{32}$$

Before extracting solutions for $U_n(\xi)$ and $V_n(\xi)$ from the earlier solutions it will be apparent to the reader that we must proceed as follows:

1. Replace temporarily the earlier quantity λ^2 by λ^2 (b/a).
2. Replace the earlier symbols a_{m1}, a_{m2}, etc., appearing after Eqs. (12) and (13) with corresponding symbols a_{n1}, a_{n2}, etc., and the symbols *emp* and *emps* by *enp* and *enps* where $enp=(2n-1)\pi/2$ and $enps=enp^2$.
3. Replace the plate aspect ratio by its inverse.

In the case of *Solution* 1 we obtain, for example (see Eqs. (25) and (26)),

$$U_n(\xi)=E_n\theta_{11n}\{\cosh\beta_n\xi+\theta_{1n}\cos\gamma_n\xi\} \tag{33}$$

and

$$V_n(\xi)=E_n\theta_{11n}\{\alpha_{2n}\sinh\beta_n\xi+\theta_{1n}\alpha_{4n}\sin\gamma_n\xi\}. \tag{34}$$

The reader will have no trouble, therefore, extracting appropriate expressions for the second building block response, from those of the first, for all three types of solution possible here:

Before moving on to set up the eigenvalue matrix for the symmetric–symmetric family of modes it is preferable to first obtain solutions for the response of the building blocks utilized in analyzing the other two mode families.

2.2. The anti-symmetric–anti-symmetric mode family

Free vibration analysis for this mode family, discussed earlier, is achieved by means of the building blocks represented in Fig. 4. The quarter plate of interest is shown to the left of the figure. It will be recalled that the plate displacement normal to the ξ- and η-axis now has an anti-symmetric distribution with respect to these axes.

Edges $\xi=1$, and $\eta=1$, of the first building block are again free of shear stress and the edge $\eta=1$, is driven by a distributed imposed harmonic normal stress.

A Levy-type solution for the first building block can be written as

$$U(\xi,\eta)=\sum_{m=1,2}^{\infty} U_m(\eta)\sin(m-1)\pi\xi \tag{35}$$

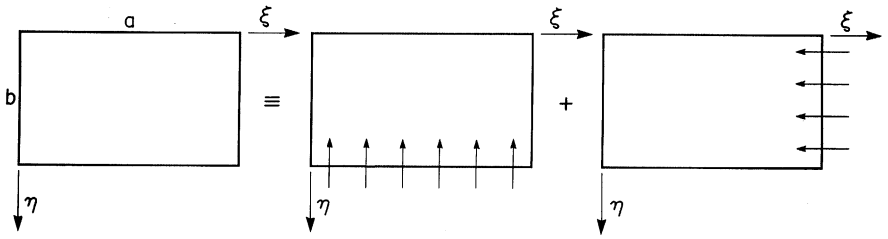

Fig. 4. Schematic representation of quarter plate and building blocks utilized in anti-symmetric–anti-symmetric mode analysis.

and

$$V(\xi,\eta)=\sum_{m=1,2}^{\infty} V_m(\eta)\cos(m-1)\pi\xi. \tag{36}$$

Substituting in the governing differential equations, in a manner identical to that followed in analysis of the symmetric–symmetric modes, we again arrive at the equilibrium equations (12) and (13) where now

$$a_{m1}=\frac{a_{66}}{\phi^2},\quad b_{m1}=\frac{-emp(a_{66}+a_{12})}{\phi},\quad c_{m1}=\lambda^4-a_{11}\,emps,$$

$$a_{m2}=\frac{a_{11}}{\phi^2},\quad b_{m2}=\frac{emp(a_{12}+a_{66})}{\phi},\quad c_{m2}=\lambda^4-a_{66}\,emps,$$

where $emp=(m-1)\pi$, and $emps=emp^2$.

Again, the quantity $V_m(\eta)$ is governed by Eq. (14) and the three possible solution forms for $V_m(\eta)$ are as given by Eqs. (16)–(18). The principal difference here relates to the solution term when subscript m equals 1, i.e., emp, b_{m1}, and b_{m2} equal zero. There is then no contribution to the quantity $U_m(\eta)$ (Eq. (35)). From Eq. (13) we obtain

$$V_m^{||}(\eta)+\alpha^2 V_m(\eta)=0, \tag{37}$$

where

$$\alpha^2=\frac{\lambda^4\phi^2}{a_{11}}.$$

The solution for Eq. (37) is well known and, since $V_m(\eta)$ is anti-symmetric about the ξ-axis, we have

$$V_m(\eta)=A_0\sin\alpha\eta. \tag{38}$$

The amplitude of the dimensionless harmonic driving stress along the edge $\eta=1$ is expressed in series form as

$$\sigma_y^*(\xi)=\sum_{m=1,2}^{\infty} E_m\cos(m-1)\pi\xi. \tag{39}$$

Taking the solution for $V_m(\eta)$ (Eq. (38)) and enforcing Eq. (39), ($m = 1$), we obtain,

$$V_m(\eta) = E_m \frac{\phi}{\alpha \cos \alpha} \sin \alpha\eta. \tag{40}$$

The response of the building block to the first driving term is thus completely established.

Turning now to the building block response to driving terms with $m > 1$, it is seen that we must proceed in a manner identical to that described for the symmetric–symmetric modes. The only difference is that now, for each of the three solution forms, terms related to displacement V and symmetric about the ξ-axis must be deleted. Only the results thereby obtained are presented here.

Case 1: Solution 1 applicable

$$V_m(\eta) = E_m\theta_{11m}\{\sinh \beta_m\eta + \theta_{1m} \sin \gamma_m\eta\}, \tag{41}$$

$$U_m(\eta) = E_m\theta_{11m}\{\alpha_{1m} \cosh \beta_m\eta + \theta_{1m}\alpha_{3m} \cos \gamma_m\eta\}, \tag{42}$$

where

$$\theta_{11m} = \frac{1.}{[\beta_m/\phi + \nu\, emp\, \alpha_{1m}]\cosh \beta_m + \theta_{1m}[\gamma_m/\phi + \nu\, emp\, \alpha_{3m}]\cos \gamma_m},$$

$$\theta_{1m} = \frac{[\beta_m\alpha_{1m} - \phi\, emp]\sinh \beta_m}{[\gamma_m\alpha_{3m} + \phi\, emp]\sin \gamma_m},$$

$$\alpha_{1m} = \beta_m(a_{m1}a_{m2}\beta_m^2 + a_{m1}c_{m2} - b_{m1}b_{m2})/c_{m1}b_{m2},$$

$$\alpha_{3m} = -\gamma_m(a_{m1}a_{m2}\gamma_m^2 - a_{m1}c_{m2} + b_{m1}b_{m2})/c_{m1}b_{m2},$$

Case 2: Solution 2 applicable

$$V_m(\eta) = E_m\theta_{11m}\{\sin \beta_m\eta + \theta_{1m} \sin \gamma_m\eta\} \tag{43}$$

and

$$U_m(\eta) = E_m\theta_{11m}\{\alpha_{1m} \cos \beta_m\eta + \theta_{1m}\alpha_{3m} \cos \gamma_m\eta\}, \tag{44}$$

where

$$\theta_{11m} = \frac{1}{\{[\beta_m/\phi + \nu\, emp\, \alpha_{1m}]\cos \beta_m + \theta_{1m}[\gamma_m/\phi + \nu\, emp\, \alpha_{3m}]\cos \gamma_m\}},$$

$$\theta_{1m} = \frac{-(\alpha_{1m}\beta_m + \phi\, emp)\sin \beta_m}{(\alpha_{3m}\gamma_m + \phi\, emp)\sin \gamma_m},$$

$$\alpha_{1m} = -\beta_m\{a_{m1}a_{m2}\beta_m^2 - a_{m1}c_{m2} + b_{m1}b_{m2}\}/c_{m1}b_{m2},$$

$$\alpha_{3m} = -\gamma_m\{a_{m1}a_{m2}\gamma_m^2 - a_{m1}c_{m2} + b_{m1}b_{m2}\}/c_{m1}b_{m2}.$$

Case 3: Solution 3 applicable

$$V_m(\eta) = E_m\theta_{11m}\{\sinh \beta_m\eta + \theta_{1m} \sinh \gamma_m\eta\} \tag{45}$$

and

$$U_m(\eta) = E_m\theta_{11m}\{\alpha_{1m} \cosh \beta_m(\eta) + \theta_{1m}\alpha_{3m} \cosh \gamma_m\eta\}, \tag{46}$$

where

$$\theta_{11m} = \frac{1.}{\{[\beta_m/\phi + v\,emp\,\alpha_{1m}]\cosh\beta_m + \theta_{1m}[\gamma_m/\phi + v\,emp\,\alpha_{3m}]\cosh\gamma_m\}},$$

$$\theta_{1m} = \frac{-[\alpha_{1m}\beta_m - \phi\,emp]\sinh\beta_m}{[\alpha_{3m}\gamma_m - \phi\,emp]\sinh\gamma_m},$$

$$\alpha_{1m} = \beta_m[a_{m1}a_{m2}\beta_m^2 + a_{m1}c_{m2} - b_{m1}b_{m2}]/c_{m1}b_{m2},$$

$$\alpha_{3m} = \gamma_m[a_{m1}a_{m2}\gamma_m^2 + a_{m1}c_{m2} - b_{m1}b_{m2}]/c_{m1}b_{m2}.$$

The solution for the response of the second building block of Fig. 4 is extracted from that of the first. The procedure to be followed is completely analogous to that described in connection with the symmetric–symmetric mode analysis.

2.3. The symmetric–anti-symmetric mode family

Free vibration analysis of this mode family is achieved by means of the building blocks represented in Fig. 5. Focusing on the first building block it is seen that it differs from that employed in the previous mode study (Fig. 4), only that now terms in the solution for $V_m(\eta)$ which are anti-symmetrically distributed about the ξ-axis must be deleted. All other quantities are unchanged. This minor difference is easily implemented. Solutions for the quantities $U(\xi,\eta)$ and $V(\xi,\eta)$ are again as given by Eqs. (33) and (34). It is shown that solutions for these quantities are as follows.

For the first term in the expansions, $m = 1$,

$$V_m(\eta) = \frac{-E_m\phi}{\alpha\sin\alpha}\cos\alpha\eta. \tag{47}$$

For $m > 1$, the following solutions apply:

Case 1: Solution 1 applicable

$$V_m(\eta) = E_m\theta_{11m}(\cosh\beta_m\eta + \theta_{1m}\cos\gamma_m\eta), \tag{48}$$

$$U_m(\eta) = E_m\theta_{11m}\{\alpha_{2m}\sinh\beta_m\eta + \theta_{1m}\alpha_{4m}\sin\gamma_m\eta\}, \tag{49}$$

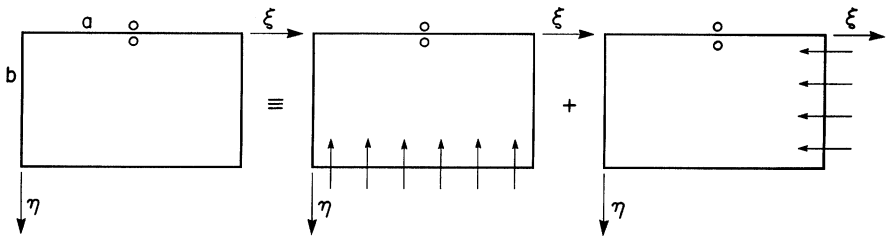

Fig. 5. Schematic representation of quarter plate and building blocks utilized in analyzing modes symmetric with respect to the ξ-axis and anti-symmetric with respect to the η-axis.

where

$$\theta_{11m} = \frac{1.}{[\beta_m/\phi + v\ emp\ \alpha_{2m}]\sinh\beta_m - \theta_{1m}[\gamma_m/\phi - v\ emp\ \alpha_{4m}]\sin\gamma_m},$$

$$\theta_{1m} = -\frac{[\beta_m\alpha_{2m} - \phi\ emp]\cosh\beta_m}{[\gamma_m\alpha_{4m} - \phi\ emp]\cos\gamma_m},$$

$$\alpha_{2m} = \beta_m(a_{m1}a_{m2}\beta_m^2 + a_{m1}c_{m2} - b_{m1}b_{m2})/c_{m1}b_{m2},$$

$$\alpha_{4m} = \gamma_m(a_{m1}a_{m2}\gamma_m^2 - a_{m1}c_{m2} + b_{m1}b_{m2})/c_{m1}b_{m2}.$$

Case 2: Solution 2 applicable

$$V_m(\eta) = E_m\theta_{11m}\{\cos\beta_m\eta + \theta_{1m}\cos\gamma_m\eta\} \tag{50}$$

and

$$U_m(\eta) = E_m\theta_{11m}\{\alpha_{2m}\sin\beta_m\eta + \theta_{1m}\alpha_{4m}\sin\gamma_m\eta\}, \tag{51}$$

where

$$\theta_{11m} = \frac{-1}{\{[\beta_m/\phi - v\ emp\ \alpha_{2m}]\sin\beta_m + \theta_{1m}[\gamma_m/\phi - v\ emp\ \alpha_{4m}]\sin\gamma_m\}},$$

$$\theta_{1m} = \frac{-(\alpha_{2m}\beta_m - \phi\ emp)\cos\beta_m}{(\alpha_{4m}\gamma_m - \phi\ emp)\cos\gamma_m},$$

$$\alpha_{2m} = \beta_m\{a_{m1}a_{m2}\beta_m^2 - a_{m1}c_{m2} + b_{m1}b_{m2}\}/c_{m1}b_{m2},$$

$$\alpha_{4m} = \gamma_m\{a_{m1}a_{m2}\gamma_m^2 - a_{m1}c_{m2} + b_{m1}b_{m2}\}/c_{m1}b_{m2}.$$

Case 3: Solution 3 applicable

$$V_m(\eta) = E_m\theta_{11m}\{\cosh\beta_m\eta + \theta_{1m}\cosh\gamma_m\eta\} \tag{52}$$

and

$$U_m(\eta) = E_m\theta_{11m}\{\alpha_{2m}\sinh\beta_m(\eta) + \theta_{1m}\alpha_{4m}\sinh\gamma_m\eta\}, \tag{53}$$

where

$$\theta_{11m} = \frac{1.}{\{[\beta_m/\phi + v\ emp\ \alpha_{2m}]\sinh\beta_m + \theta_{1m}[\gamma_m/\phi + v\ emp\ \alpha_{4m}]\sinh\gamma_m\}},$$

$$\theta_{1m} = \frac{-[\alpha_{2m}\beta_m - \phi\ emp]\cosh\beta_m}{[\alpha_{4m}\gamma_m - \phi\ emp]\cosh\gamma_m},$$

$$\alpha_{2m} = \beta_m[a_{m1}a_{m2}\beta_m^2 + a_{m1}c_{m2} - b_{m1}b_{m2}]/c_{m1}b_{m2},$$

$$\alpha_{4m} = \gamma_m[a_{m1}a_{m2}\gamma_m^2 + a_{m1}c_{m2} - b_{m1}b_{m2}]/c_{m1}b_{m2}.$$

Finally, we examine the second building block of Fig. 5. It will be obvious that a solution for this second building block cannot be obtained from that of the first through a transformation of axes.

It is found advantageous here to introduce an intermediate building block from which the desired solution can be obtained through such a transformation. Consider the first building block of Fig. 3, utilized in symmetric–symmetric mode analysis. Let us consider the solution for a building block, identical to this except that the displacement V is anti-symmetrically distributed about the ξ-axis. Such a solution is easily obtained. We let this modified building block act as the intermediate one. It is seen that the solution is readily transformed to provide the desired solution for the second building block of Fig. 5.

Solution for the displacements U and V will be as given by Eqs. (10) and (11). It is found that the quantities $V_m(\eta)$ and $U_m(\eta)$ are as follows.

Case 1: Solution 1 applicable

$$V_m(\eta) = E_m\theta_{11m}(\sinh\beta_m\eta + \theta_{1m}\sin\gamma_m\eta), \tag{54}$$

$$U_m(\eta) = E_m\theta_{11m}\{\alpha_{1m}\cosh\beta_m\eta + \theta_{1m}\alpha_{3m}\cos\gamma_m\eta\}, \tag{55}$$

where

$$\theta_{11m} = \frac{1.}{[\beta_m/\phi - \nu\, emp\,\alpha_{1m}]\cosh\beta_m + \theta_{1m}[\gamma_m/\phi - \nu\, emp\,\alpha_{3m}]\cos\gamma_m},$$

$$\theta_{1m} = \frac{[\beta_m\alpha_{1m} + \phi\, emp]\sinh\beta_m}{[\gamma_m\alpha_{3m} - \phi\, emp]\sin\gamma_m},$$

$$\alpha_{1m} = \beta_m(a_{m1}a_{m2}\beta_m^2 + a_{m1}c_{m2} - b_{m1}b_{m2})/c_{m1}b_{m2},$$

$$\alpha_{3m} = -\gamma_m(a_{m1}a_{m2}\gamma_m^2 - a_{m1}c_{m2} + b_{m1}b_{m2})/c_{m1}b_{m2}.$$

Case 2: Solution 2 applicable

$$V_m(\eta) = E_m\theta_{11m}\{\sin\beta_m\eta + \theta_{1m}\sin\gamma_m\eta\} \tag{56}$$

and

$$U_m(\eta) = E_m\theta_{11m}\{\alpha_{1m}\cos\beta_m\eta + \theta_{1m}\alpha_{3m}\cos\gamma_m\eta\}, \tag{57}$$

where

$$\theta_{11m} = \frac{1}{\{[\beta_m/\phi - \nu\, emp\,\alpha_{1m}]\cos\beta_m + \theta_{1m}[\gamma_m/\phi - \nu\, emp\,\alpha_{3m}]\cos\gamma_m\}},$$

$$\theta_{1m} = \frac{-(\alpha_{1m}\beta_m - \phi\, emp)\sin\beta_m}{(\alpha_{3m}\gamma_m - \phi\, emp)\sin\gamma_m},$$

$$\alpha_{1m} = -\beta_m\{a_{m1}a_{m2}\beta_m^2 - a_{m1}c_{m2} + b_{m1}b_{m2}\}/c_{m1}b_{m2},$$

$$\alpha_{3m} = -\gamma_m\{a_{m1}a_{m2}\gamma_m^2 - a_{m1}c_{m2} + b_{m1}b_{m2}\}/c_{m1}b_{m2}.$$

Case 3: Solution 3 applicable

$$V_m(\eta) = E_m\theta_{11m}\{\sinh\beta_m\eta + \theta_{1m}\sinh\gamma_m\eta\} \tag{58}$$

and

$$U_m(\eta) = E_m\theta_{11m}\{\alpha_{1m}\cosh\beta_m\eta + \theta_{1m}\alpha_{3m}\cosh\gamma_m\eta\}, \tag{59}$$

where

$$\theta_{11m} = \frac{1.}{\{[\beta_m/\phi - v\,emp\,\alpha_{1m}]\cosh\beta_m + \theta_{1m}[\gamma_m/\phi - v\,emp\,\alpha_{3m}]\cosh\gamma_m\}},$$

$$\theta_{1m} = \frac{-[\alpha_{1m}\beta_m + \phi\,emp]\sinh\beta_m}{[\alpha_{3m}\gamma_m + \phi\,emp]\sinh\gamma_m},$$

$$\alpha_{1m} = \beta_m[a_{m1}a_{m2}\beta_m^2 + a_{m1}c_{m2} - b_{m1}b_{m2}]/c_{m1}b_{m2},$$

$$\alpha_{3m} = \gamma_m[a_{m1}a_{m2}\gamma_m^2 + a_{m1}c_{m2} - b_{m1}b_{m2}]/c_{m1}b_{m2}.$$

The solution for the response of the second building block of Fig. 5 is obtained, of course, by transformation of the above solution according to the rules introduced earlier. Solutions for the response of all building blocks employed in free in-plane vibration analysis of the completely free plate are now available.

2.4. Development of the eigenvalue matrix

Eigenvalue matrices for the mode families discussed here are generated in a manner completely analogous to that followed in analyzing free lateral vibration modes of the same plate [4]. First, for each mode family the associated pair of building block solutions are superimposed, one-upon-the-other. Following this operation, driving coefficients appearing in the building block solutions are so constrained that net normal stresses along the edges, $\eta = 1$, and $\xi = 1$, are caused to vanish. This is achieved for each edge by first expanding the contributions toward normal stress, of each of the building blocks, in an appropriate series of K terms, where K equals the number of terms utilized in the building block solutions. Following this operation, each of the net coefficients in the new boundary series, of K terms, is set equal to zero. This results in the generation of a set of K homogeneous algebraic equations involving the $2K$ driving coefficients. Since there are two driven edges, there will be a total of $2K$ equations relating the $2K$ unknown coefficients. The coefficient matrix of the combined set of equations becomes our eigenvalue matrix. A computer search is made to find those non-zero values of the parameter, λ^2, which cause the determinant of the eigenvalue matrix to vanish. These values of λ^2 are our sought-after eigenvalues. With any eigenvalue established, one of the non-zero driving coefficients associated with this eigenvalue matrix is set equal to unity. The resulting set of non-homogeneous algebraic equations is then solved to evaluate the other driving coefficients. Following this step the mode shape associated with the eigenvalue is plotted.

Here, we briefly describe steps involved in the generation of the eigenvalue matrix for symmetric–symmetric modes, only. A schematic representation of the matrix, based on three-term expansions of the building block solutions is provided in Fig. 6. Small inserts to the right of the figure indicate the boundary condition to be addressed. It is immediately seen to be advantageous to expand the normal stress contributions of the building blocks toward the edge, $\eta = 1$, in a sine series as utilized in Eq. (24). Focusing now on the contributions toward the first term in the boundary series, as represented schematically in the first row of elements in the matrix, we note that the contribution of the first building block is already available in this series. Turning toward the contribution of the second building block we find that each term in its solution contributes

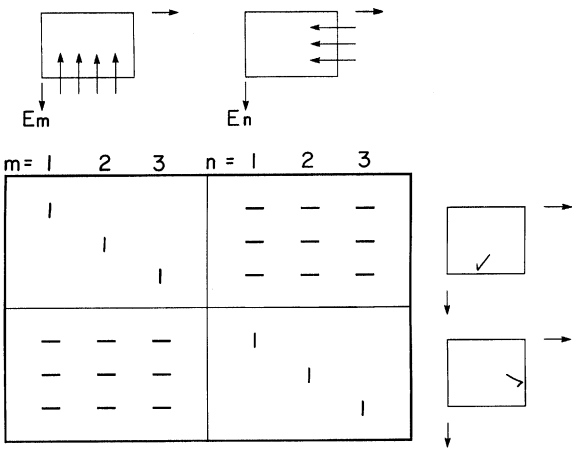

Fig. 6. Schematic representation of the eigenvalue matrix based on 3-term building block solutions.

toward the first term in the boundary series. These contributions, associated with E_n, $n = 1, 2, 3$, are easily obtained utilizing standard known integrals and are represented by short dashed lines. The second and third row of elements in the matrix are established in an identical manner. They pertain, of course, to the second and third terms in the boundary series. It will be noted that the upper left quadrant of the matrix is composed of diagonal terms only, each equal to unity.

The lower half of the matrix is generated in an identical fashion. Here, the quadrant with diagonal terms only, will be on the right hand side. In the case of a square plate it will be found, for symmetric–symmetric, as well as anti-symmetric–anti-symmetric, mode analysis, that elements of the lower left quadrant of the matrix are identical to those of the upper right. This will not be the case when conducting symmetric–anti-symmetric mode analysis. Following the above steps the eigenvalue matrices are generated for each of the three distinct mode families.

3. Presentation of computed results

The first step to be taken in the analysis at hand is to check convergence rates and decide how many terms to utilize in the building block solutions. It is also necessary to decide upon how many significant digits are required in the computed eigenvalues. It was agreed to follow practices related to lateral plate vibration and compute eigenvalues correct to four significant digits.

In Table 1 computed results are tabulated for the first symmetric–symmetric mode eigenvalue of in-plane vibration of a square plate. These eigenvalues were computed to five significant digits for various values of K, the number of terms utilized in the building block solutions. The Poisson ratio was assigned a value of 0.3 for all computations related to the present paper.

It is seen that there is a very high rate of convergence. Increasing the value of K beyond three does not change even the fifth digit in the computed eigenvalues. As a result of convergence behaviour observed in Table 1, as well as findings related to other tests, it was decided to adopt a value of eleven for the parameter K, for all computed data reported here. This is probably much higher than that required to obtain four significant digits in the eigenvalues.

Table 1
Computed eigenvalues vs. K for first symmetric–symmetric mode of square plate ($\nu = 0.3$)

K	λ^2	K	λ^2
3	1.1603	9	1.1603
5	1.1603	11	1.1603
7	1.1603	13	1.1603

Table 2
First four symmetric–symmetric mode eigenvalues computed for completely free square plate

Mode	λ^2	
	Present	Ref. [2]
1	1.160	1.160
2	2.153	1.314
3	2.629	—
4	2.643	—

Table 3
First four anti-symmetric–anti-symmetric mode eigenvalues computed for the completely free square plate

Mode	λ^2	
	Present	Ref. [1]
1	1.314	1.494
2	1.494	1.726
3	1.726	—
4	2.523	—

Tabulated eigenvalues computed for the first four symmetric–symmetric free in-plane vibration modes of the completely free square plate are presented in Table 2.

Where possible, the present results are compared with those of Bardell et al. [1]. It is seen that agreement between the two sets of data is excellent. The third mode for a square plate is reported as being an anti-symmetric–anti-symmetric mode in Ref. [1] with an eigenvalue of 1.314. It is virtually certain that it is, in fact, a symmetric–symmetric mode as reported here.

Computed eigenvalues for the first four anti-symmetric–anti-symmetric modes of the square plate are tabulated in Table 3. Again excellent agreement between the present results and those of Ref. [1] is obtained.

Computed results related to a study of symmetric–anti-symmetric mode vibration of the completely free square plate are tabulated in Table 4.

It will be appreciated that each of these computed eigenvalues represent ‘double eigenvalues’. An additional mode shape, anti-symmetric with respect to the ξ-axis and symmetric with respect to the η-axis, is attached to each computed eigenvalue. This is why in Ref. [1] a double eigenvalue has been uncovered with two distinct mode shapes attached to it. From a computational point of

Table 4
Computed first four eigenvalues for the completely free square plate*

Mode	λ^2	
	Present	Ref. [1]
1	1.236	1.236
2	1.862	—
3	2.485	—
4	3.050	—

*Modes are symmetric with respect to the ξ-axis and anti-symmetric with respect to the η-axis.

Table 5
First four symmetric–symmetric mode eigenvalues for completely free rectangular plate, $\varphi = 0.5$

Mode	λ^2	
	Present	Ref. [1]
1	1.634	1.634
2	2.363	2.363
3	3.428	—
4	3.974	—

Table 6
First four anti-symmetric–anti-symmetric mode eigenvalues for completely free rectangular plate, $\varphi = 0.5$

Mode	λ^2	
	Present	Ref. [1]
1	1.480	1.480
2	2.604	2.603
3	3.074	—
4	3.298	—

view an advantage of separating out the mode shape families through analyzing the quarter plate, as is done here, lies in the fact that only distinct eigenvalues are uncovered. There will be a well-defined crossing of the axis, at each eigenvalue, when the 'matrix determinant vs. trial eigenvalue' curve is plotted. Excellent agreement between the two sets of data is again observed.

Eigenvalues have also been computed for a rectangular plate with an aspect ratio, b/a, of 0.5. Computed eigenvalues for the first four symmetric–symmetric modes of this completely free plate are tabulated in Table 5. A corresponding set of eigenvalues are presented in Table 6 for the anti-symmetric–anti-symmetric mode family.

Very good agreement is again obtained between the two sets of data.

Further computed eigenvalues for the same plate of aspect ratio 0.5 are tabulated in Table 7. The associated mode shapes are either symmetric with respect to the ξ-axis and anti-symmetric

Table 7
First four computed eigenvalues for free vibration modes symmetric about the ξ-axis and anti-symmetric about the η-axis (symbol S-A), or symmetric about the η-axis and anti-symmetric about the ξ-axis (symbol A-S), $\varphi = 0.5$

Mode	λ^2		Mode type
	Present	Ref. [1]	
1	0.9779	0.977	S-A
2	2.392	—	S-A
3	2.629	—	A-S
4	2.685	—	A-S

with respect to the η-axis, as discussed earlier, or anti-symmetric with respect to the ξ-axis and symmetric with respect to the η-axis. It will be appreciated that modes of the second family are easily analyzed by utilizing the 'symmetric–anti-symmetric' mode analysis technique described earlier with the plate aspect ratio replaced by its inverse. This is what has been done in the present study.

Again, very good agreement between eigenvalues computed here and those of Ref. [1] is encountered. The only difference of significance relates to the second eigenvalue of Table 7, i.e., the one related to the first mode, anti-symmetric with respect to the ξ-axis and symmetric with respect to the η-axis. This eigenvalue appears not to have been uncovered in the study reported in Ref. [1]

4. Conclusions

As indicated at the beginning, the main purpose of this paper has been to introduce the superposition method as a means for the obtaining of highly accurate analytical type solutions for the free in-plane vibration of rectangular plates. The completely free rectangular plate has been arbitrarily selected as the vehicle for demonstrating this capability.

Proceeding in a manner analogous to that followed in rectangular plate free lateral vibration analysis, it has been shown that the method lends itself equally well to solution of in-plane problems. The problem of trying to select functions to represent in-plane displacements is eliminated. The governing differential equations are satisfied exactly and boundary conditions are satisfied to any desired degree of accuracy. Convergence is rapid and excellent agreement is obtained when computed eigenvalues are compared with those obtained earlier by the Rayleigh–Ritz energy approach.

Demonstration that the superposition method works so well in the solution of in-plane problems, as is done here, constitutes an important step forward. It will certainly be applicable to vast families of more complicated in-plane problems such as those related to point supported plates, plates with in-plane elastic support, and plates with local attached masses, etc. It is hoped to extend the method to handle such problems in future work.

Appendix. Nomenclature

a, b rectangular plate edge lengths
E Youngs modulus of plate material

G_{xy}	modulus of elasticity in shear of plate material
t	time
u, v	plate in-plane displacements in x and y directions, respectively
U, V	dimensionless displacements $U = u/a,\ V = v/a$
x, y	rectangular plate co-ordinates
ξ, η	dimensionless co-ordinates $\xi = x/a$, and $\eta = y/b$
φ	plate aspect ratio, b/a
$\sigma_x, \sigma_y, \tau_{xy}$	normal in-plane stresses in x and y directions and in-plane shear stress, respectively
$\sigma_x^*, \sigma_y^*, \tau_{xy}^*$	dimensionless in-plane normal and shear stresses, defined in text
ω	circular frequency of plate vibration
ρ	mass density of plate material
v	Poisson ratio of plate material (taken here as 0.3)
λ^2	dimensionless frequency of plate vibration, $\lambda^2 = \omega a\sqrt{\rho(1 - v^2)/E}$

References

[1] N.S. Bardell, R.S. Langley, J.M. Dunsdon, On the free in-plane vibration of isotropic rectangular plates, *Journal of Sound and Vibration* 191 (3) (1996) 459–467.

[2] Y. Kobayshi, G. Yamada, S. Honma, In-plane vibration of point-supported rectangular plates, *Journal of Sound and Vibration* 126 (3) (1988) 545–549.

[3] R.H. Gutierrez, P.A.A. Laura, In-plane vibration of thin elastic rectangular plates elastically restrained against translation along the edges, *Journal of Sound and Vibration* 132 (3) (1989) 512–515.

[4] D.J. Gorman, Free vibration analysis of the completely free rectangular plate by the method of superposition, *Journal of Sound and Vibration* 57 (1978) 432–447.